Chapter – 3

Microstructural Refinement of an Interstitial-free Steel Processed by Equal-Channel Angular Pressing

3.1 Effect of ECAP on Microstructural Refinement

Microstructure of coarse grained as-received interstitial-free steel (Figure 3.1(a)) consists of single phase nearly equiaxed ferrite grains of average size 57.6±21 μm. At ε_{vm}=0.6, the grains get elongated (Figure 3.1(b)), shown by single arrow). The refinement process begins by shearing of grains into the deformation bands (Figure 3.1b, shown by double arrows). At ε_{vm}=1.2, dislocation density increases further and thickness of deformation bands decreases (Figure 3.1(c)). At ε_{vm}=1.8, recovery of dislocations takes place and cell blocks get aligned to deformation direction. At this strain grain size is reduced so much that it is only partially revealed by optical microscopy (Figure 3.1(d)).

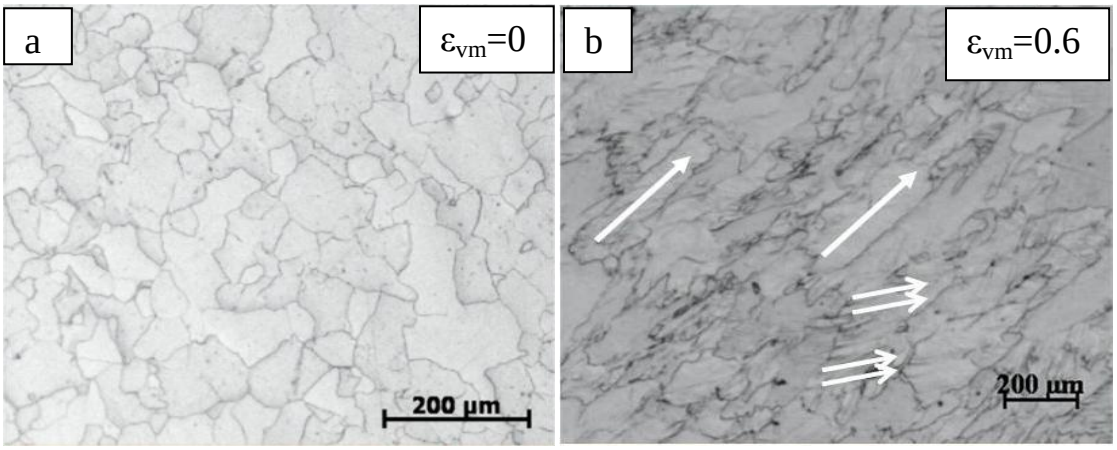

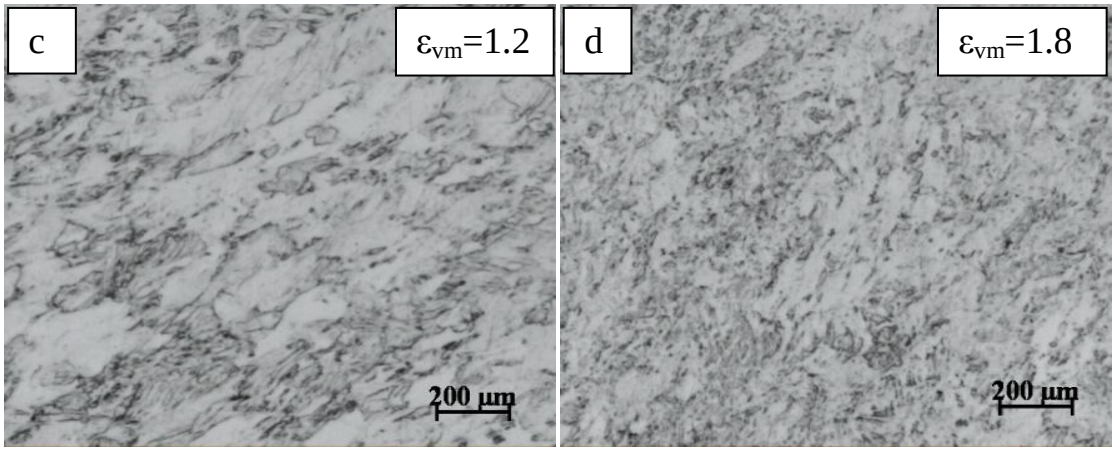

Figure 3.1: Optical micrographs of samples at (a) ε_{vm}=0, (b) ε_{vm}=0.6, (c) ε_{vm}=1.2, (d) ε_{vm}=1.8.

Reference frames for as-received rolled IF steel and ECAPed material are displayed in Figures 2.6 a2, a3. Figures 3.2(a)-(m) show the image quality maps where high angle and low angle grain boundaries are delineated by blue color lines and red color lines respectively. Majority of the boundaries of as-received IF steel are of high angle boundaries (Figure 3.2(a)). At ε_{vm}=0.6, the structure becomes banded one with high defect density (Figure 3.2(b)). Therefore, HAGB fraction decreases to 0.1. At ε_{vm}=1.2, the band thickness has reduced (Figure 3.2(c)) and HAGB fraction further decreases to 0.08. The cells have formed inside the bands by a dynamic recovery process at ε_{vm}=1.8 (Figure 3.2(d)). Through ε_{vm}=0.6 to 1.8 the boundaries are partially revealed due to high dislocation density. The enlarged view is from the same location where it is superimposed. At ε_{vm}=2.4, the bands are aligned in the deformation direction and the cells are formed in deformation bands (Figure 3.2(e)) and HAGB fraction increases to 0.15. At ε_{vm}=3, the band thickness is further reduced, the intersection of bands can be seen in the IQ map with the decreased length of the band as well (Figure 3.2(f)). The deformation induced high angle grain boundaries (HAGBs) are shown in the enlarged

view in the similar way as above in the inset of the behind location. HAGB fraction increases to 0.24.

At ε_{vm}=6, the original high angle boundaries, band boundaries, cell block boundaries align themselves along the deformation direction leading to the lamellar structure. One lamellae is shown by two arrows in the inset magnified area and the location is indicated by single arrow (Figure 3.2(g)). HAGB fraction increases to 0.41. With increase in strain, the spacing of lamellae decreases to one or two subgrains wide at a few places at ε_{vm}=9 and form ribbon grains (Figure 3.2(h)). Similar highly deformed bands for aluminium alloys with very high aspect ratio were named as ribbon grains advocated by Prangnell et al. [Prangnell 2004]. The HAGB fraction increases to 0.56. At ε_{vm}=12, the microstructure is fully converted to ribbon grains (Figure 3.2(i)). At ε_{vm}=15, the ribbon grains are sheared into near-equiaxed grains which also contain subgrains (Figure 3.2(j)). The fragmentation continues till ε_{vm}=18 and the effective grain size decreases (Figure 3.2(k)). HAGB fraction reaches a saturation value of 0.66. At ε_{vm}=21, the grains are near-equiaxed shape. Nature of the grain boundary and the shape of grains are shown in the inset from the location shown by arrow (Figure 3.2(l)). At ε_{vm}=24, grains are also near-equiaxed shape. The majority of the grain boundaries are of high angle grain boundaries which are shown in the inset whose location is indicated by the single arrow (Figure 3.2(m)).

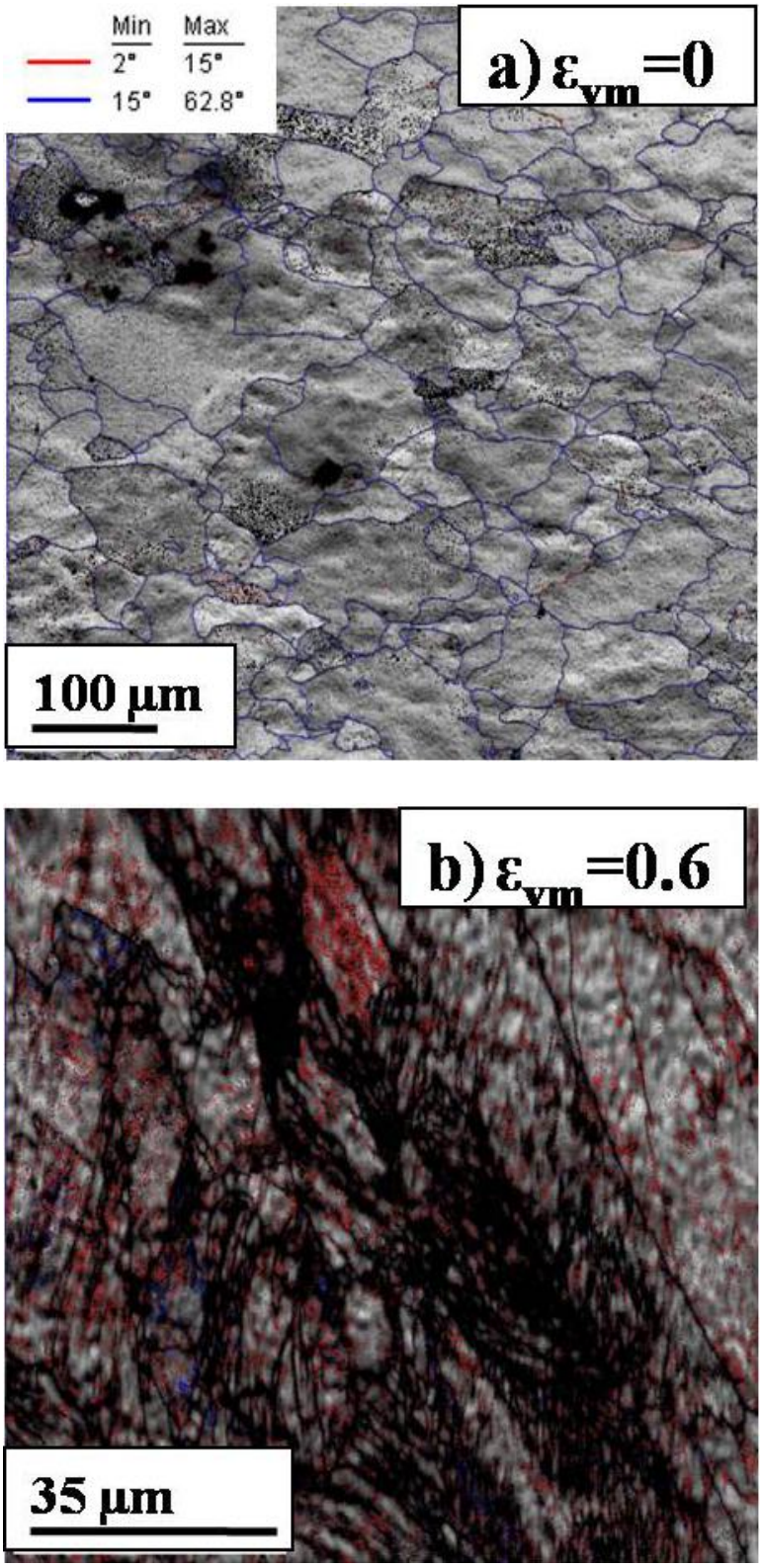

Figure 3.2: Image quality maps of IF steel of (a) ε_{vm}=0 and (b) ε_{vm}=0.6, Blue and red lines delineate high angle grain boundaries and low angle grain boundaries respectively.

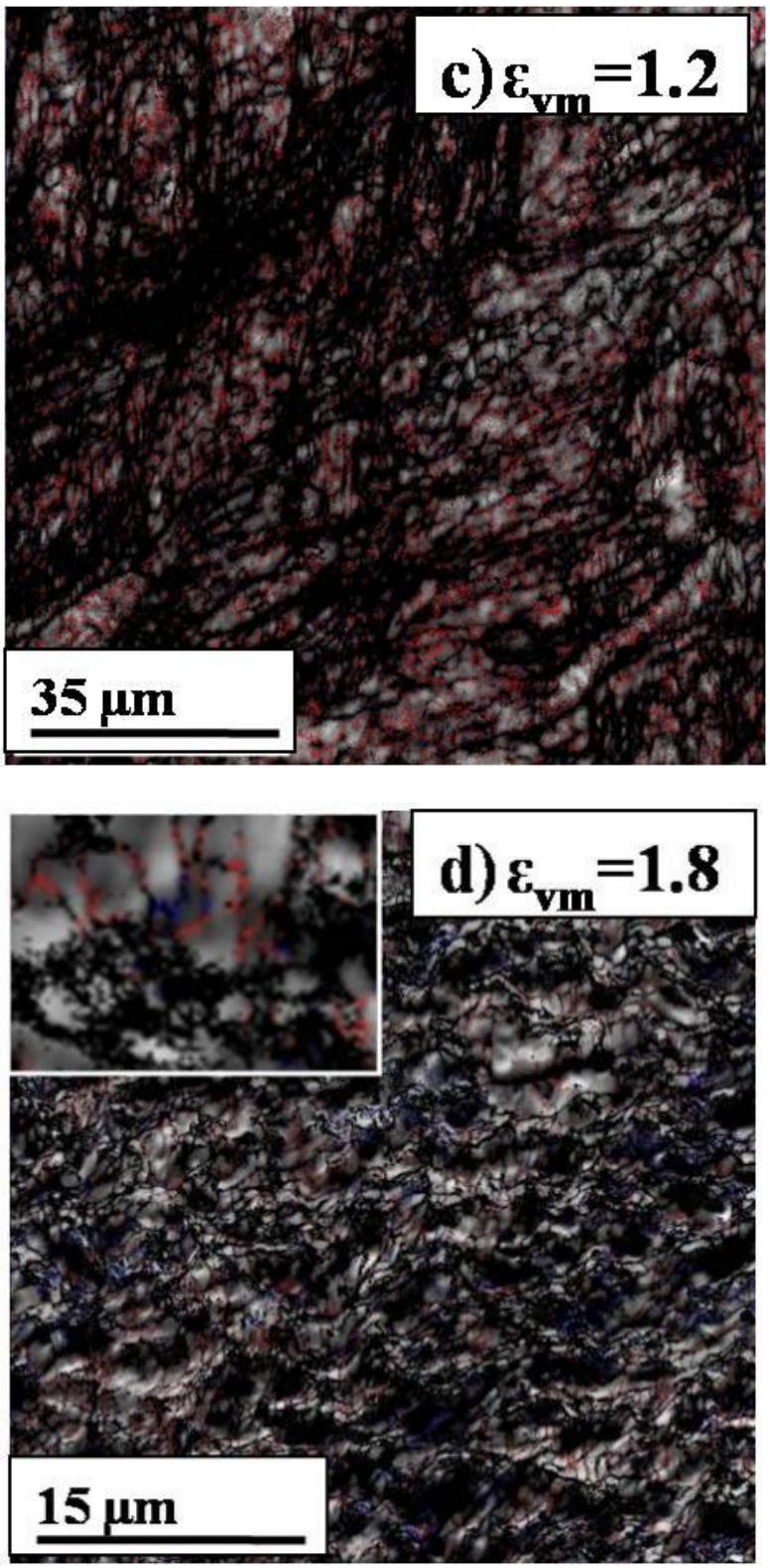

Figure 3.2: Image quality map of IF steel of (c) ε_{vm}=1.2 and (d) ε_{vm}=1.8, Magnified view of selected area is given on corresponding Figure with an arrow at left hand top corner for selected strains.

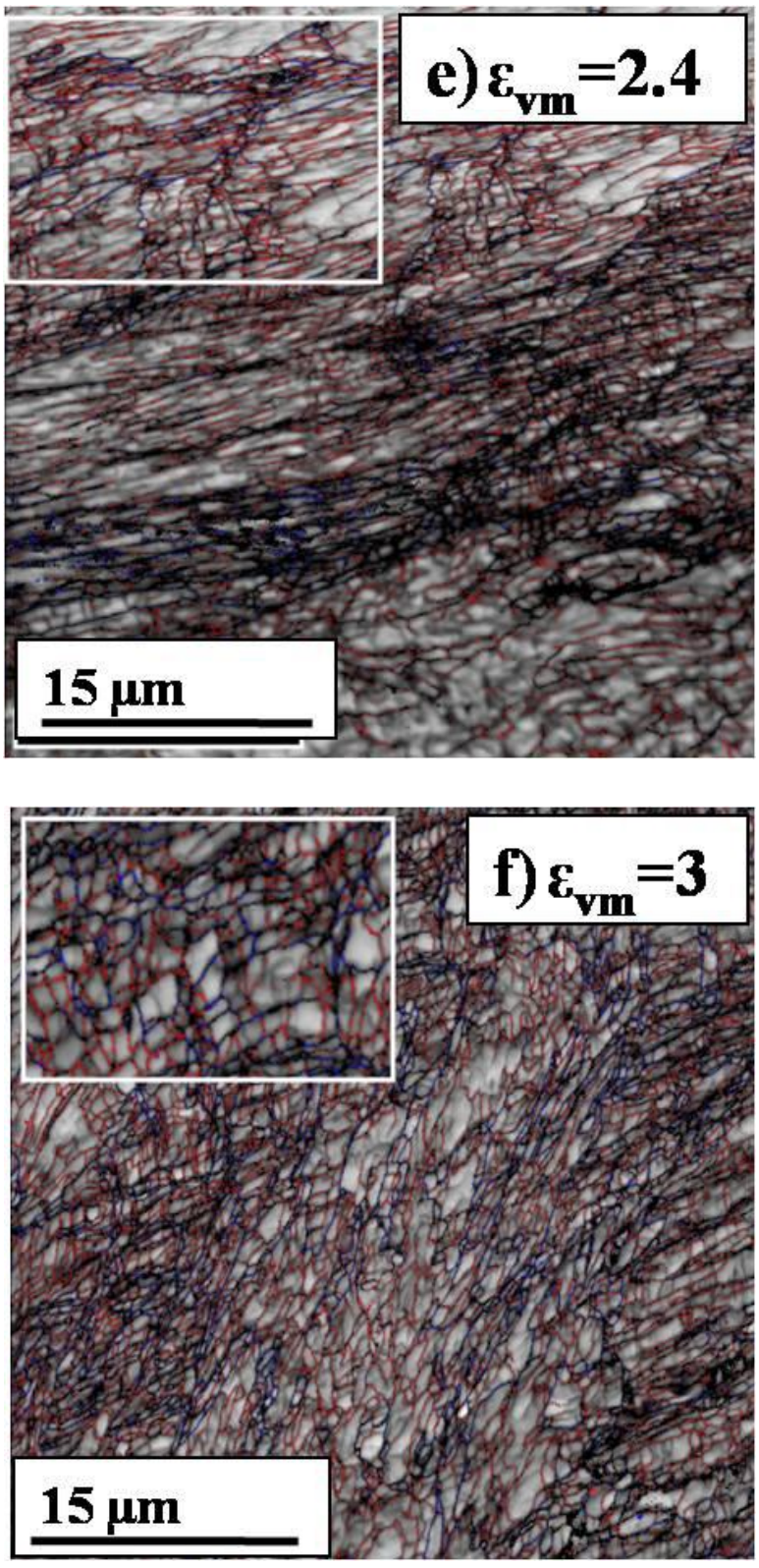

Figure 3.2: Image quality maps of IF steel of (e) ε_{vm}=2.4 and (f) ε_{vm}=3.

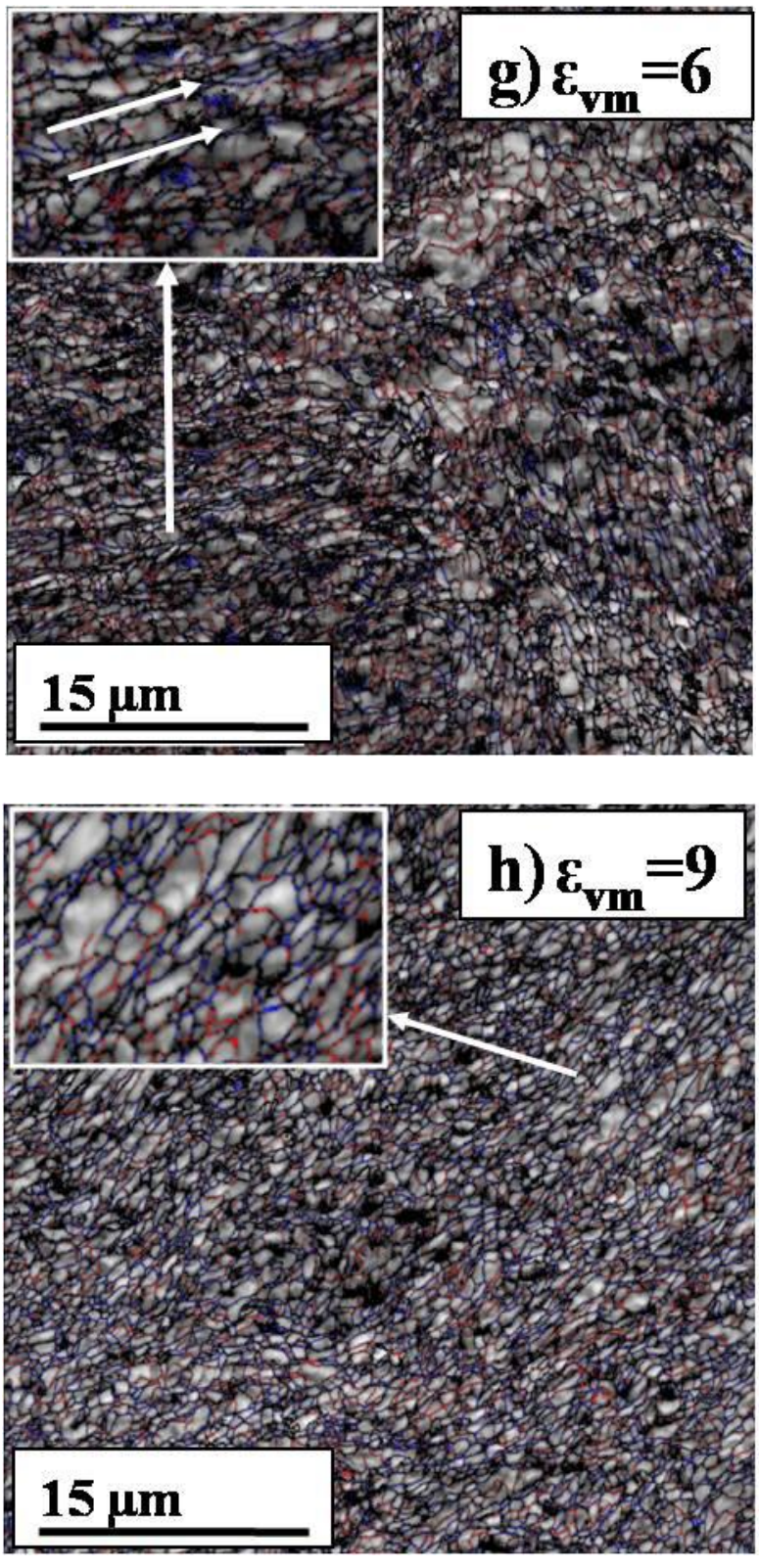

Figure 3.2: Image quality maps of IF steel of (g) ε_{vm}=6 and (h) ε_{vm}=9.

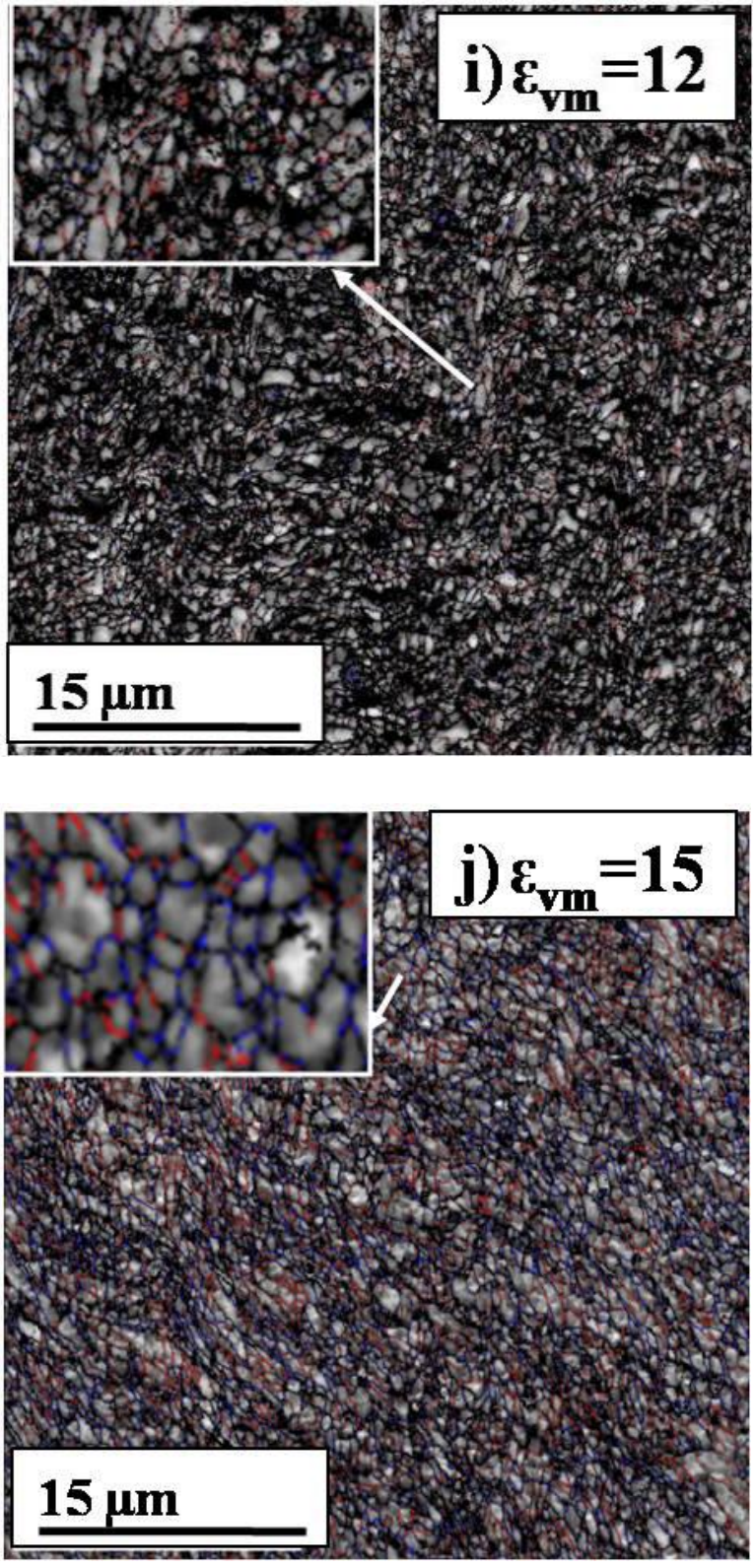

Figure 3.2: Image quality maps of IF steel of (i) ε_{vm}=12 and (j) ε_{vm}=15.

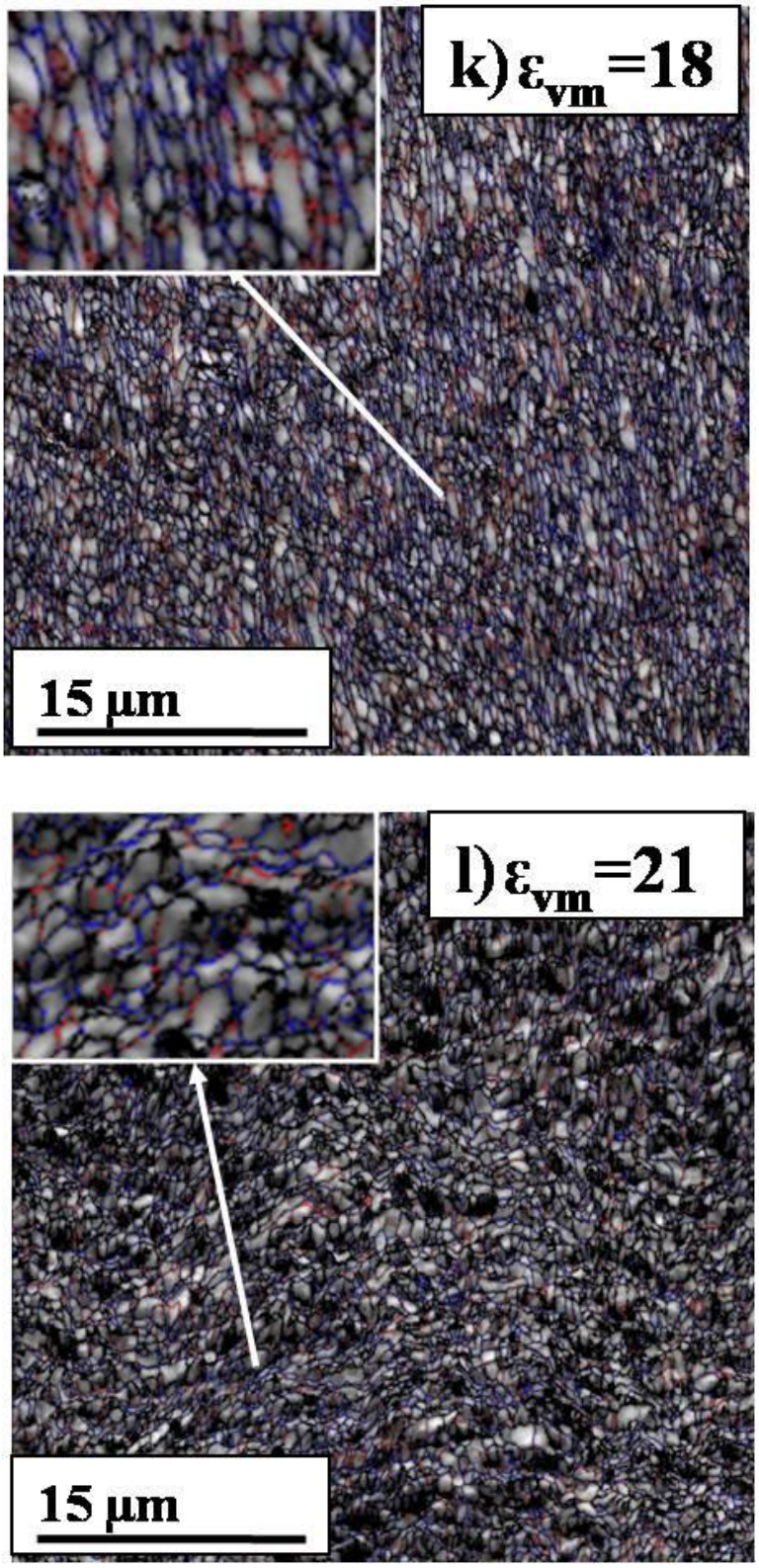

Figure 3.2: Image quality maps of IF steel of (k) ε_{vm}=18 and (l) ε_{vm}=21.

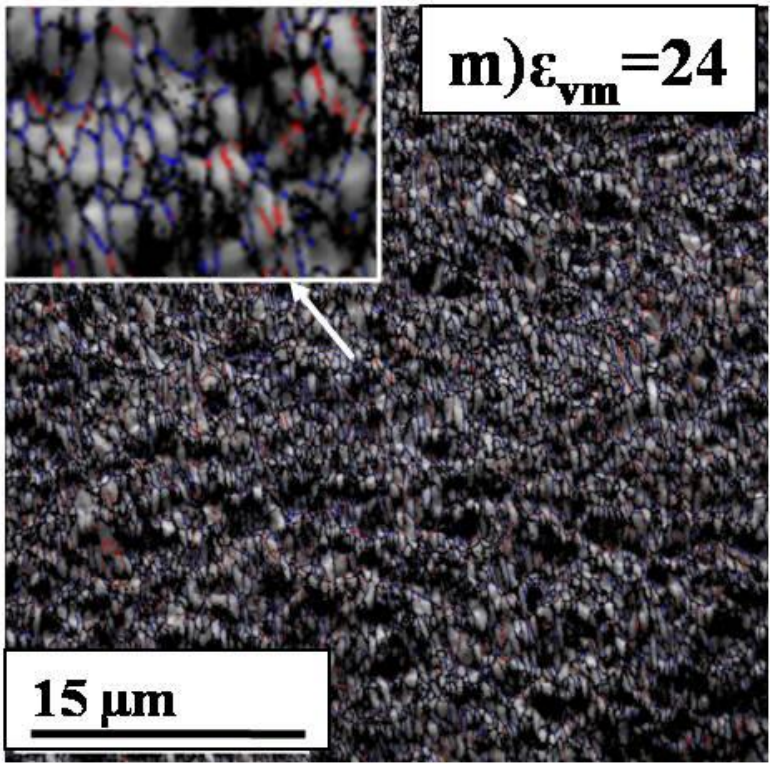

Figure 3.2: Image quality map of IF steel of (m) ε_{vm}=24.

Figures 3.3(a)-(l) show the TEM bright field images of IF steel at the various strains (ε_{vm}). Here grain size was measured by optical micrographs using Heyn's lineal intercept method. Microstructure of as-received sample (Figure 3.3(a)) shows the equiaxed ferrite grains of an average size of 57.6±21 µm. Interior of grains are dislocation free and boundary of grains are sharp indicative of high angle of misorientation. At ε_{vm}=0.6, deformation bands of average width 395±36 nm are formed having high dislocation density. At ε_{vm}=1.2, the thickness of the deformation bands decreases to 354±34 nm and dislocation density further increases (Figure 3.3c). Figure 3.3(c), shows that the boundary of the deformation band which is parallel to $[\bar{2}2\bar{2}]$ and plane of boundary is (110). The cell structures are formed in bands through the dislocation rearrangement by a dynamic recovery process, at ε_{vm}=1.8 (Figure 3.3(d)). At

an initial deformation state, the grains get subdivided into regions of different orientations and the thick boundaries of the deformation bands consist of the transition bands which comprise of cells having width of one cell. The thin boundaries of the deformation bands are deformation-induced grain boundaries. In course of deformation, the misorientation between the bands increases and that sharpens the boundary. At ε_{vm}=2.4, the boundaries of bands reach to high angle of misorientation and the grain size is reduced simultaneously (Figure 3.3(e)). At low to medium strain (ε_{vm}=1.8–2.4) the cell blocks started aligning to the deformation directions.

On further increasing strain to ε_{vm}=3, the bands get aligned towards the deformation direction and the thickness of band decreases (Figure 3.3(f)). The intersection of different bands formed between two orthogonal directions of deformation results from two successive passes. At ε_{vm}=6, the high angle boundaries (original high angle boundaries, boundaries of deformation bands and some of cell block boundaries) get aligned to the deformation direction producing lamellar structures (shown by arrow in the inset of Figure 3.3(g)) where inset is from the location shown by arrow. With an increase in strain lamellar width decreases to the width of one to two subgrains at ε_{vm}=9 (Figure 3.3(h)) and form ribbon grains. Even beyond ε_{vm}=9, the cell size decreases (upto ε_{vm}=12). The width of the ribbon grains decreases and finally becomes almost to that of single subgrain wide (width of ribbon grain is 196 nm) (Figure 3.3(i)). The ribbon grains get sheared partially into near-equiaxed grains at ε_{vm}=12. At large ε_{vm}=15, the ribbon grains split into the near-equiaxed grains (Figure 3.3(j)) with some of the subgrains inside and fragmentation continues with increasing strain till ε_{vm}=18. Through ε_{vm}=21 to 24, the

grain size remains almost unchanged and the shape is also near-equiaxed (Figure 3.3(k)-(l)). The equiaxed HAGBs are shown in the inset from the location shown by arrow.

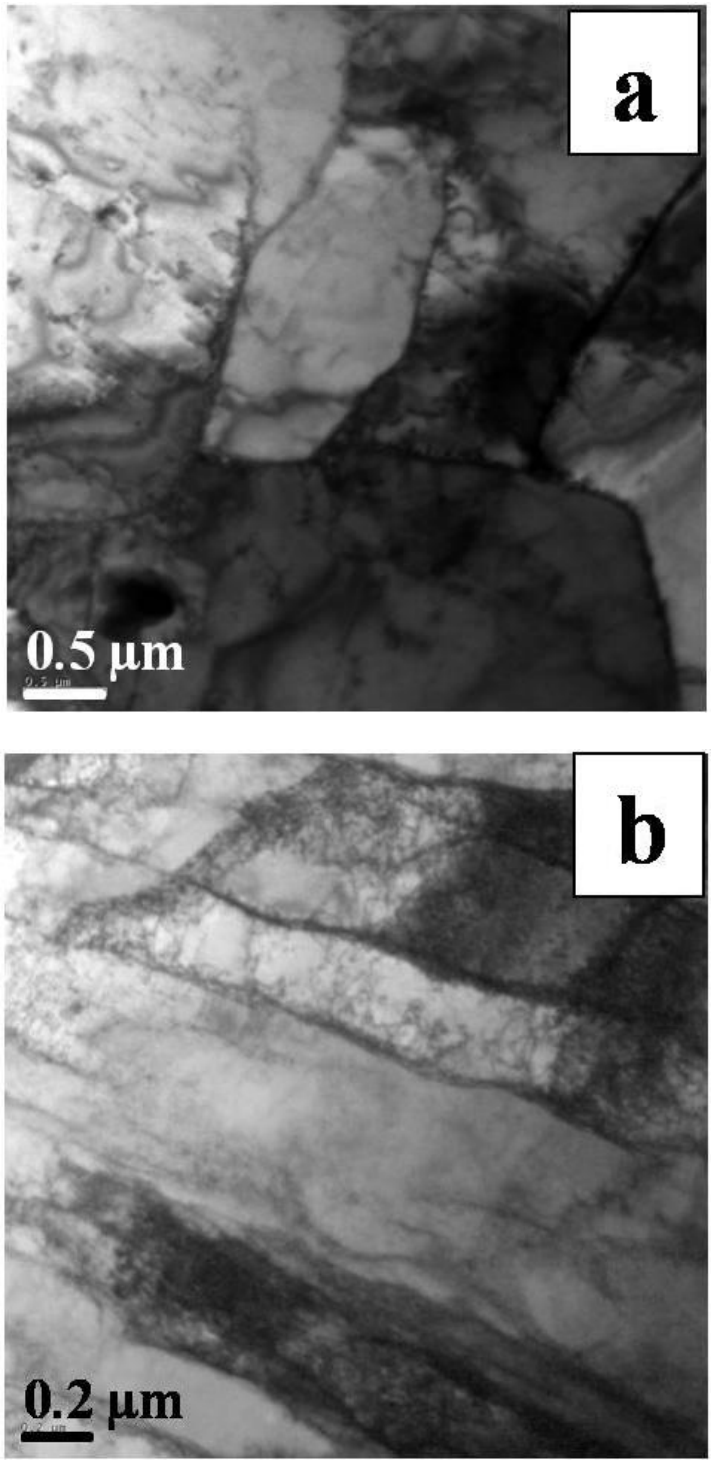

Figure 3.3: TEM bright field images of IF steel after ECAP for (a) ε_{vm}=0 and (b) ε_{vm}=0.6.

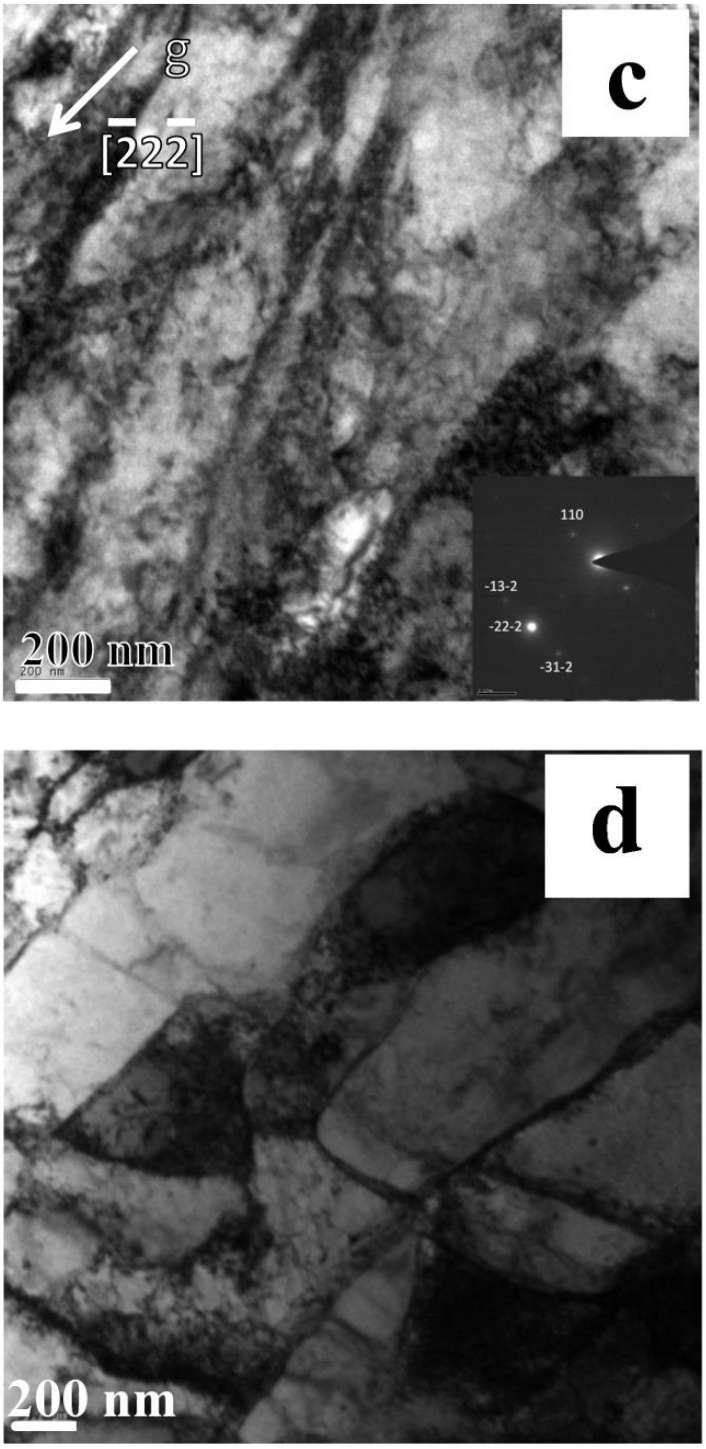

Figure 3.3: TEM bright field images of IF steel after ECAP for and (c) ε_{vm}=1.2 and (d) ε_{vm}=1.8. indexed selected area diffraction patterns are displayed at the corner of the respective bright field image.

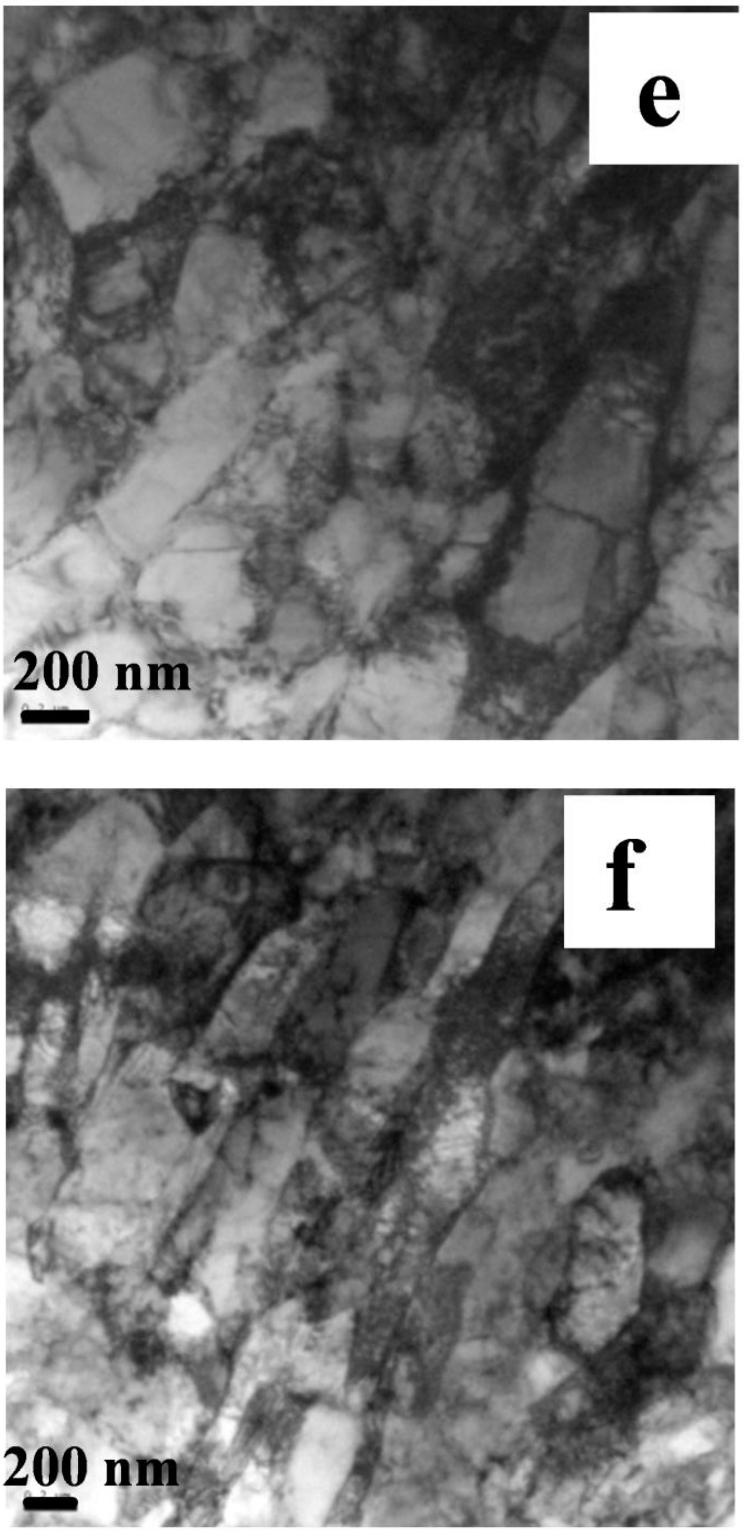

Figure 3.3: TEM bright field images of IF steel after ECAP for and (e) ε_{vm}=2.4 and (f) ε_{vm}=3.

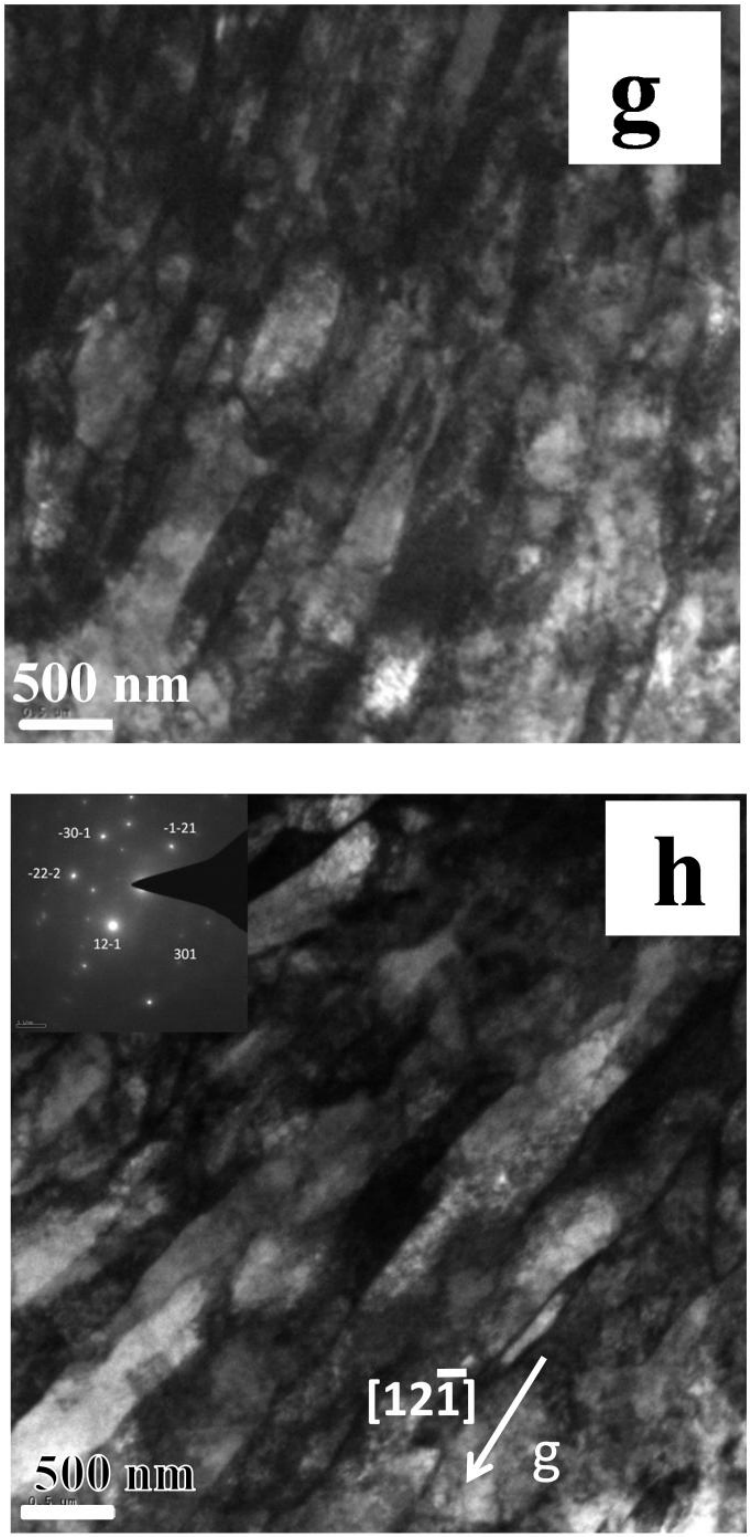

Figure 3.3: TEM bright field images of IF steel after ECAP for and (g) ε_{vm}=6 and (h) ε_{vm}=9.

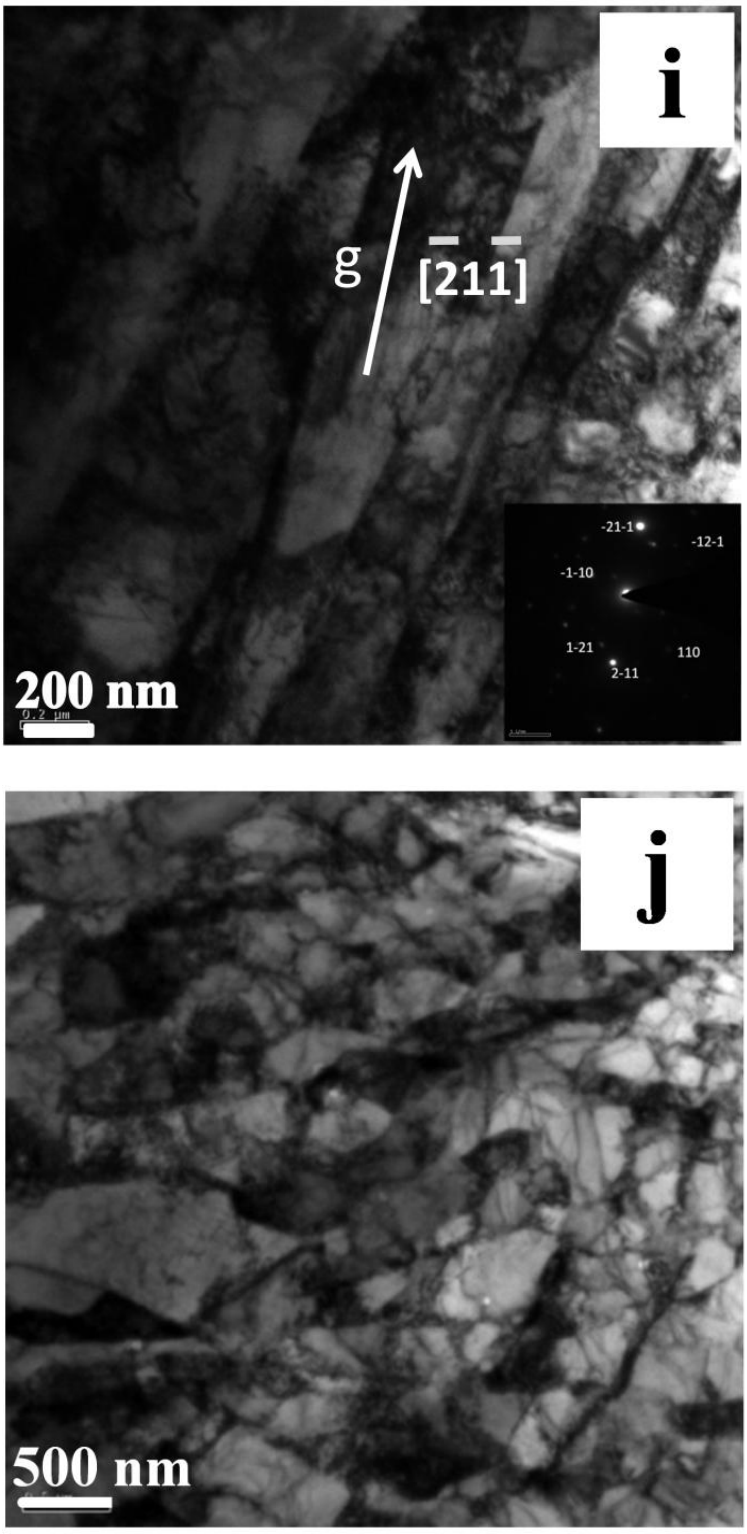

Figure 3.3: TEM bright field images of IF steel after ECAP for and (i) ε_{vm}=12 and (j) ε_{vm}=15.

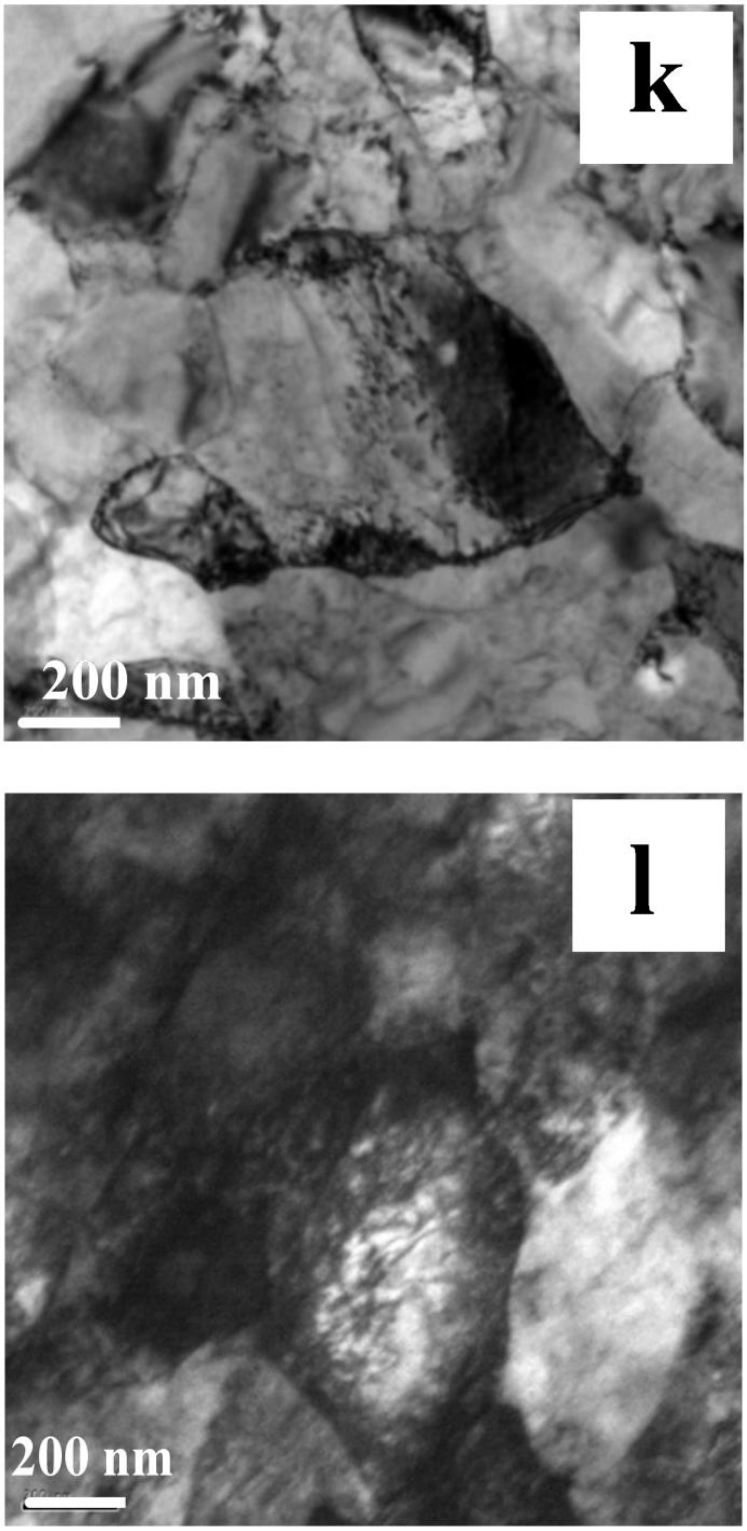

Figure 3.3: TEM bright field images of IF steel after ECAP for (k) ε_{vm}=21 and (l) ε_{vm}=24.

Figure 3.4 shows the variation of the grain size, errors in measurement with increasing strain. The grain refinement takes place at a rapid rate at the initial stage of the deformation ε_{vm}=0-3. Through ε_{vm}=0 to 1.2, the dislocation density increases and the grain refinement takes place by elongation of the grains and subdivision of grains to bands. At ε_{vm}=1.8, the cell formation takes place by a dynamic recovery process and thinning of bands. At ε_{vm}=2.4, thinning of bands continues. At ε_{vm}=3, bands are fragmented by intersection between two orthogonal directions. The cell size decreases at a low rate after ε_{vm}=3 or rate of grain refinement slows down (ε_{vm}=3-18). There after, it remains almost constant through ε_{vm}=21 to 24. At this stage, no further formation of the cells takes place but the high angle grain boundary fraction increases. Even after ε_{vm}=24, microstructure contains significant amount of dislocations and the microstructure is metastable.

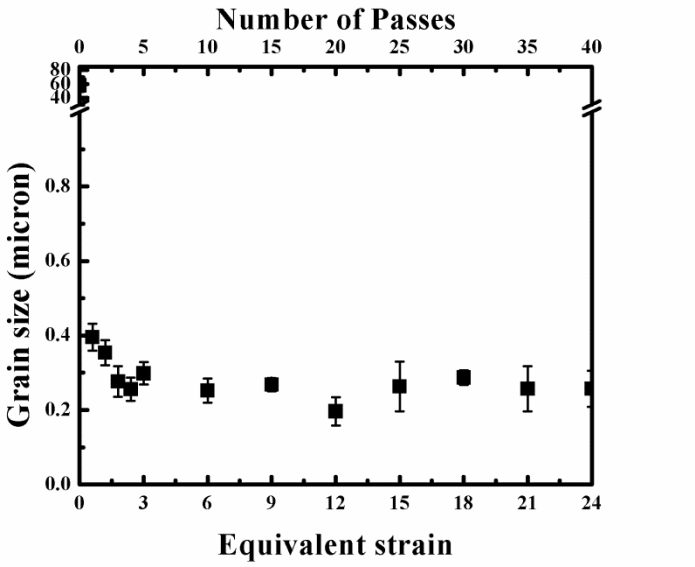

Figure 3.4: Variation of grain size (measured from TEM images) with equivalent strain.

Figure 3.5 (a) shows the variation of low angle grain boundaries (LAGB) fraction with ε_{vm}. In as-received sample, majority of boundaries are HAGBs with small fraction of

LAGBs (0.116). At ε_{vm}=0.6, the LAGB increases to 0.90. Highest value of 0.92 of LAGBs are observed at ε_{vm}=1.2. However grain boundaries are partially revealed from equivalent strain 0.6 to 1.8 due to highly strained matrix because of high dislocation density. At ε_{vm}=9, LAGB reaches to ~0.44. At ε_{vm}>9, it continues to decrease and reaches to a saturated value of 0.34 at ε_{vm}=18. Through ε_{vm}=21 to 24 it remains almost unchanged. Figure 5(b) shows the variation of average misorientation angle with increasing strain. Average misorientation angle is highest in the as-received material (~37°). At ε_{vm}=1.2 it reaches a minimum value of 6° but there after increases continuously and reaches ~24° at ε_{vm}=9. With further increase in strain average misorientation angle builds up and reaches a maximum value of 28° at large strain ε_{vm}>18. Table 3.1 gives the microstructural parameters and mechanical properties of all deformed specimens.

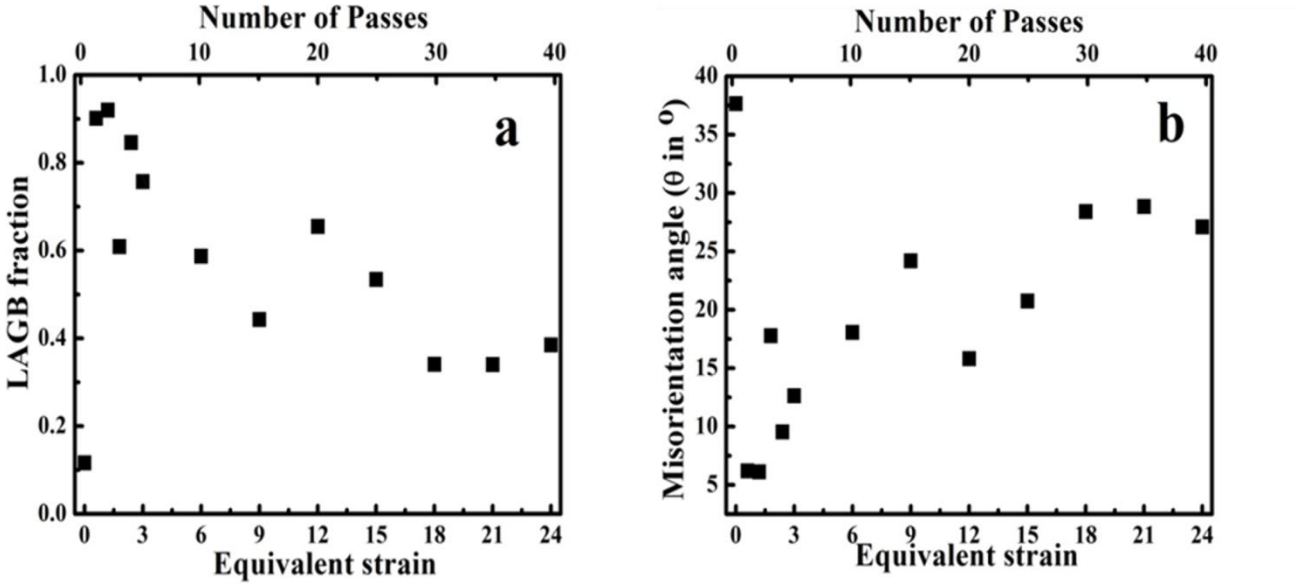

Figure 3.5: Variation of (a) low angle grain boundary fraction and (b) average misorientation angle with equivalent strain (ε_{vm}) in IF steel. Data points are joined by dotted line to show trend.

3.2 Discussion

The coarse grained equiaxed microstructure (Figure 3.1(A)) of as-received IF steel, get elongated and split into deformation bands at just one pass of ECAP or equivalent strain of 0.6 with high density of dislocations and the grain size is decreased. The boundaries of deformation bands are low angle boundaries with increased LAGB fraction and therefore, average misorientation angle decreases to a lowest value. However, grain boundaries are partially revealed at equivalent strain 0.6 to 1.8 due to high dislocation density. With increase in strain to 1.2, bands are elongated and the band thickness decreases (Figure 3.1(b),3.2(c)). In the bands, the dislocation density increases and LAGB fraction reaches to approximately a maximum (Figure 3.5(a)) value and thereby the average misorientation angle becomes minimum. Through ε_{vm}=1.8 to 2.4, (Figure 3.2(c)), cells are formed in the bands separated by the rotational dislocation boundaries due to the dynamic recovery process. A few cells are separated by a thick cell block boundaries. There is an attendant increase in the misorientation angle and thereby decrease in LAGB fraction (Figure 3.5(a)-(b)). In addition, the bands get aligned in deformation direction. At ε_{vm}=3, the intersection of different bands formed between two orthogonal deformation direction fragments the grain into smaller grains (Figure 3.2f). At ε_{vm}=6, the original HAGBs, boundaries of bands and some of the cell block boundaries get aligned to deformation direction and that results lamellar structures and average misorientation angle increases.

With the increase in strain the lamellar width decreases and that produces ribbon shaped grains partially. The width of each of the ribbon grains is about one or two subgrains wide at ε_{vm}=9 (Figure 3.3(h)) at few locations. Figure 3.3(h) shows that $[12\bar{1}]$

is parallel to the boundary of the ribbon grains. Thus, slip has occurred on $(12\bar{1})$ plane. The width of ribbon grains becomes almost one subgrain size at large strain ε_{vm}=12 (Figure 3.3(i)) and their length increases to large value. The walls of ribbon grains are sharp with interconnecting boundaries. The misorientation angle of periphery of the ribbon grains and subgrain boundaries continue to increase. A significant part of the subgrain boundaries converts to a HAGB thereby HAGB fraction increases. Figure 3.3(i) shows direction of ribbon grains to be parallel$[\bar{2}1\bar{1}]$. Thus, slip has occurred on $(\bar{2}1\bar{1})$ plane. At ε_{vm}=15, the ribbon grains are completely broken (Figure 3.3(j)) and near-equiaxed grained structure is formed where the majority of the boundaries are HAGBs. LAGB fraction reaches to a saturated value of 0.34 and the average misorientation angle increases to 28° at large strain of 18 (Figure 3.5 and Table I). There after, both LAGB fraction and average misorientation angle remains unchanged. At very large strain>15, the ribbon shaped grains transform to the near-equiaxed grain structure and fragmentation continues till ε_{vm}=18. At ε_{vm}>18, grain reshaping occurs due to SIBM keeping the grain size almost remain unchanged (minor changes fall within the experimental error band). At ε_{vm}=21, near-equiaxed ultrafine-grained structure is developed progressively. However still the microstructure is metastable even at ε_{vm}=24 as the grains contain significant amount of dislocations. Application of large amount of strain will add cost significantly, therefore further processing is discouraged, but there is a scope for scientific study to continue the deformation to get stable microstructures.

Table-3.1: Details of microstructural parameters of ECAPed IF steel samples

ε_{vm}	Grain size (μm)	LAGB Fraction	HAGB Fraction	Misorientation Angle(°)
0	57.6±21	0.116	0.88	37.6
0.6	0.395±0.036	0.901	0.10	6.2
1.2	0.354±0.034	0.92	0.08	6.1
1.8	0.276±0.041	0.609	0.39	17.7
2.4	0.255±0.031	0.846	0.15	9.5
3	0.298±0.03	0.757	0.24	12.6
6	0.252±0.032	0.587	0.41	18.0
9	0.268±0.018	0.443	0.56	24.1
12	0.196±0.038	0.655	0.35	15.8
15	0.263±0.067	0.534	0.47	20.7
18	0.287±0.02	0.341	0.66	28.4
21	0.256±0.061	0.34	0.66	28.8
24	0.257±0.048	0.385	0.66	27.1

3.3 Summary

Ti+Nb stabilized coarse grained interstitial-free steel can be deformed by the equal-channel angular pressing adopting route Bc upto very large equivalent strain of 24. Grains get elongated and subdivided into bands at initial passes (ε_{vm}=0.6) of ECAP. With increasing strain (ε_{vm}=1.8) the bands split to cell blocks and finally cell blocks to cells. The width of bands and the size of cells decrease with increase in the equivalent strain. However, most of the boundaries at this stage are low angle boundaries created by the rearrangement of the dislocations (at ε_{vm}=3). The grain fragmentation is a result of grain-grain interaction as neighbouning grains exert stress on each other such that local stress varies within a grain. As a consequence, different sets of slip systems are activated in

different regions of one crystal leading to different changes in orientation. There after, the misorientation angle increases with the imposed strain by progressive lattice rotation. Major high angle boundaries (original high angle boundary, boundaries of bands and cell block boundaries) align to deformation direction and form lamellar structure at ε_{vm}=6. Inter lamellar spacing decreases with strain and finally become one subgrain wide for ribbon grains at ε_{vm}= 12. With further strain the transverse boundaries of subgrains interacted with dislocations increase its misorientation angle. At very large strain >15, the ribbon shaped grains transform to the near-equiaxed grain structure and fragmentation continues till ε_{vm}=18. At very large strain>15, the ribbon shaped grains transform to the near-equiaxed grain structure and fragmentation continues till ε_{vm}=18. At ε_{vm}>18, grain reshaping occurs due to SIBM keeping the grain size almost remain unchanged (minor changes fall within the experimental error band). Through ε_{vm}=21 to 24, the grain size remain almost unchanged. It is interesting to note that even at large equivalent strain of 24, the microstructure is metastable containing low angle grain boundary fraction of 0.34. Finally average grain size, low angle grain boundary area fraction and average misorientation angle stabilize to respective saturation values.